

Behaviour factor and displacement estimation of low-ductility precast wall system under seismic actions

Patrick L.Y. Tiong^{*1}, Azlan Adnan^{1a} and Nor H.A. Hamid^{2b}

¹Department of Structure and Materials, Faculty of Civil Engineering, Universiti Teknologi Malaysia, 81310 Skudai, Johor, Malaysia

²Faculty of Civil Engineering, Universiti Teknologi MARA, 40310 Shah Alam, Selangor, Malaysia

(Received March 18, 2013, Revised June 10, 2013, Accepted August 8, 2013)

Abstract. This paper investigated the seismic behaviour of an innovated non-ductile precast concrete wall structural system; namely HC Precast System (HCPS). The system comprises load-bearing precast wall panels merely connected only to column at both ends. Such study is needed because there is limited research information available in design codes for such structure particularly in regions having low to moderate seismicity threats. Experimentally calibrated numerical model of the wall system was used to carry out nonlinear pushover analyses with various types of lateral loading patterns. Effects of laterally applied single point load (SPL), uniformly distributed load (UDL), modal distributed load (MDL) and triangular distributed load (TDL) onto global behaviour of HCPS were identified. Discussion was focused on structural performance such as ductility, deformability, and effective stiffness of the wall system. Thus, a new method for engineers to estimate the nonlinear deformation of HCPS through linear analysis was proposed.

Keywords: low ductility; displacement factor; seismic; precast concrete wall; pushover

1. Introduction

Benefits demonstrated by precast concrete building technique over the conventional cast in-situ method have been long proven in many large constructions over the world. This is clearly revealed by the widely applicable seismic design provisions for precast structures such as those contained in International Building Codes (International Code Council 2009) and Eurocode 8 (CEN 1998). Although the advancement of precast concrete industries is highly demonstrated among developed nations such as the United States and most of the European countries, its implementation among developing countries is reportedly low. Despite strong encouragement of local governments such as those of Malaysia, the level of acceptance of the precast technology is still reportedly low (Haron *et al.* 2005, Hassim *et al.* 2009).

Hence, it has become important for the private industry to initiate relevant researches onto prospective precast system that best suits the needs of local industry. Among them is the HC

*Corresponding author, E-mail: tiong.patrick@gmail.com

^a Professor, E-mail: azelan_fka_utm@yahoo.com

^b Ph.D., E-mail: norha454@salam.uitm.edu.my

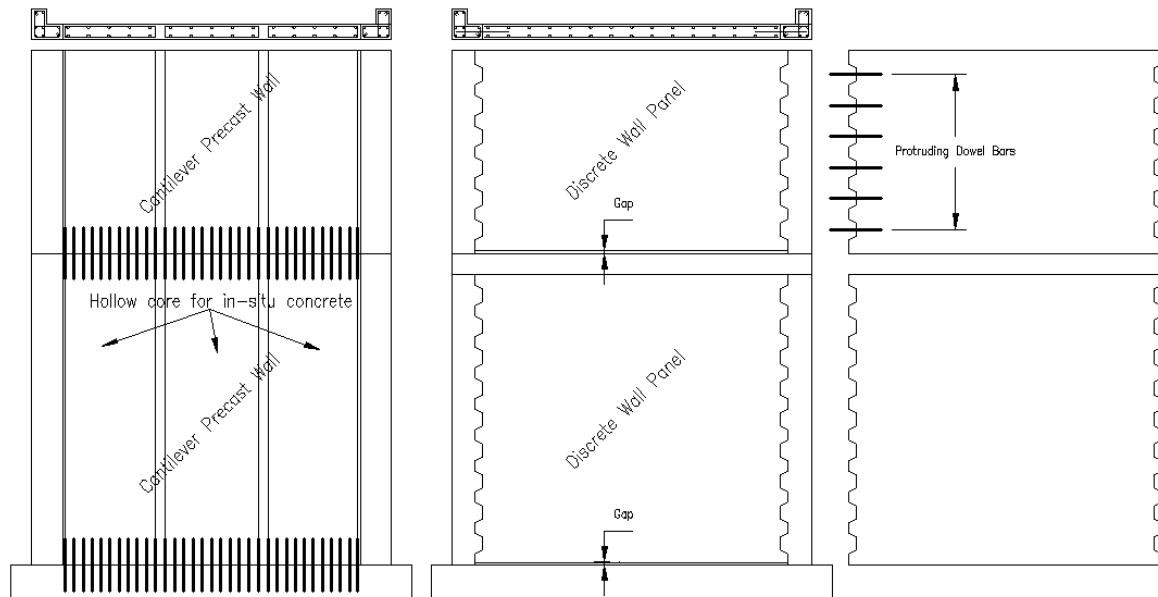


Fig. 1 (a) Cantilever wall system and (b) HC precast wall system (HCPS)

Precast System (Fig.1(b)). The system, or in short HCPS comprises load-bearing precast concrete wall panels that are connected only to the supporting cast-in-place column at both ends. There is no horizontal connectivity provided between the top and bottom wall to restrain it from sliding against each other. Due to the relatively humid and wet tropical climate of the region, wet interface provides a better water resilient capability for precast structures in the country (Hamid 2009). The proposed precast concrete wall structure is replacing the existing cantilever wall system (Fig. 1(a)). The cantilever wall system was normally made of hollow-core wall sections. The wall panels on top were connected to the bottom wall through insertion of heavier reinforcement and concreting at site. This system has been said to become unpopular among builders in recent years due to involvement of relatively heavier site works to fill in the hollow-core sections between the walls (Elliot 2002). Example of HCPS is shown in Fig. 2.

The system has been implemented in constructing more than a thousand units of residential housing as well as commercial buildings over the country. Nevertheless, the system is not designed for seismic resistant. As the country (Malaysia) is now moving forward in formulating local seismic design guidelines, it has become a necessity for the system to be analyzed accordingly in terms of seismicity effects. This paper is therefore aimed to provide research information for precast concrete wall panels analysis for regions located in low to moderate earthquake zones. As such, the final precast product will be in the range of lower ductility end; which is also termed as DCL (Ductility Class Low) in Eurocode 8 (EC8).

The early precast concrete wall construction could be traced back in the Western countries to as early as in the 60s'. Although the early construction of precast concrete structures at this point was not suitable for seismic regions, lateral forces (such as those from wind loading) have to be included in analysis and design of these structures (Bljucer 1988). Hartland (1975) recommended a simplified method in obtaining the vertical shear stress along the shear keys, which was also known as castellation interface between two adjacent wall panels. The shear stress along the height



Fig. 2 Panels of HC precast wall system

of wall panel was calculated from the difference between the stresses at upper storey and lower storey of the wall level in consideration. The margin of shear stress (or the residual shear stress) was then resisted by the shear keys along the vertical interface. Such approach clearly, assumed that these shear stresses which occurred along the vertical interface between walls were perfectly perpendicular to the direction of lateral loading. In other words, these shear keys were under direct shear demand despite the direction of lateral loading might not always be constant.

Raths (1977) and Christiansen (1973) presented step-by-step analysis and design of precast concrete load-bearing wall panels for high-rise construction in Georgia (Seismic Zone 1). The structural system for the building consisted of precast bearing wall façade in the exterior and also interior precast frame elements. The lateral loads were then, assumed to be resisted by both the frame and load-bearing wall systems, separately. The natural period of the designed building was obtained by empirical formula, and seismic design force was determined using the equivalent static force method based on the Uniform Building Code (UBC). The load-bearing walls were treated as overlapping strut with stubs elements. The interfaces between wall-to-wall and also wall-to-frame were all assumed to be perfectly rigid. At vertical interface between adjacent wall panels, interface release was carried out to allow only vertical shear stress transfer along the wall height. Such analytical method once again ruled out the possibility of any other force demand occurring at these interface locations due to seismic force. Nevertheless, this was the best effort for analysis to be possible during then. Only two types of shear stresses were considered to occur within the building. First were the horizontal shear stresses which took place at each storey level. And secondly, the vertical shear stress due to flexural behaviour (bending caused tension and

compression forces) of the building, acting like a cantilever deep beam.

Soudki *et al.* (1996) conducted a series of tests on precast concrete shear wall systems with multiple shear keys interface under lateral cyclic shear loading. The shear keys along the horizontal interface of precast concrete walls provided higher shear resistance of 3 times more than normal dry pack grouting interface. There was no reinforcing bars provided between the walls and the shear key grouting and thus, this led to high unrecoverable slip mechanism which caused overall structural instability. At higher shear loading, the dry pack grouting between shear keys cracked, and the effective shear resistance now only depended on the frictional force between the interaction surfaces.

In the effort to search for better retrofitting of non-ductile moment-resisting frame in seismic zones, Frosch *et al.* (1996) proposed the construction of precast infill walls within as additional bracing components within the frame system. The tested interface between the infill wall and the frame was unreinforced multiple shear key interfaces. The results of the study indicated that the non-ductile frame performed well under simulated cyclic loading. Nevertheless, the proposed wall systems comprised many pieces of small walls (90cm in width) connected to each other through concreting.

Despite both studies (Soudki *et al.* 1996, Frosch *et al.* 1996) were focusing on shear keys interface of precast wall panels, the orientation of the shear keys were parallel towards the direction of lateral loading. In other words, the reaction forces within the shear keys were acting towards the same direction as shear force. The effects of shear keys acting perpendicular (normal) towards shear force remains unexplored.

Rodriguez and Blandon (2005) investigated the damage behaviour of precast concrete building constructed using dual system. The dual system refers to interaction of structural walls and beam-column frames. The purpose of the study was to evaluate the global stability of the precast system under seismic loading. It was observed that the presence of reinforced concrete walls reduced the lateral displacement of concrete frames significantly. Initial yielding of the structure started from wall cracks.

Although the study revealed good displacement control of precast concrete walls, this decreased the ductility of the global structure. Lower ductility means lesser capability of the structure to deform in the post-elastic range without significant degradation of strength, stiffness and energy dissipation. Ductility plays a very important role in absorbing shocks and forces from strong ground motion (Englekirk 2003). Therefore, by introducing a kind of semi-rigid interface between the wall and frame elements, the ductility of the overall structure can be increased, which is one of the objectives in this current research. Besides, the interfaces between wall-to-foundation and wall-to-beam were all monolithically fixed. The test results showed formation of plastic hinges away from the interfaces. Hence, the study was concentrating more onto the damage of structural elements themselves rather than on their interfaces, since all interfaces were rigidly fixed.

A study by Divan and Madhkhan (2011) revealed that the behaviour factor (q_0) or also-known-as response modification factor (R_f) could easily be affected by the presence of wall panels, and also the height of structure. The authors made use of the shear key results tested by Chakrabati *et al.* (1988).

2. Research significance

The currently available seismic design provisions allow for several simplified analysis method

besides the conventional nonlinear dynamic time history analyses which often face numerical instability and are time consuming. Among the said simplified method is the nonlinear pushover analysis. In the pushover analysis, some lateral loading is applied onto the structure until instability occurs or the ultimate deformation capacity is reached. The designers will then be able to determine the global capacity curve of the specific structure. Nevertheless, there is neither single guideline nor code provision to recommend the lateral loading pattern that approximates the behaviour of a structure, particularly those associated with low natural period structure. Taking for example, EC8 recommends usage of two lateral loading patterns; namely the uniformly distributed load (UDL) and modal pushover analysis (MPA). There are also researchers proposing TDL, triangular distributed load (Pecker 2007, Vafaei *et al.* 2011). To add matter worse, behaviour and characteristics of precast interface under seismic effects are rather complex and must be seriously taken into account during the design phase (Lu *et al.* 2012). Therefore, this paper aims to investigate the influence of these different lateral loading patterns onto the nonlinear response of low period precast concrete wall panels. Thus, a simplified procedure will then be recommended for engineers to estimate the nonlinear displacement of the structure by only applying linear analysis.

3. The structural model (HCPS)

In order to reduce the amount of site works to encourage the system usage, the precast wall panels are reinforced with minimal reinforcement detailing as required by British Standard BS 8110-1997 (British Standards Institution 1997). As the BS code has been superseded by European Codes and the country is currently moving towards that, the provided reinforcement is also checked to satisfy Eurocode 2 (CEN 1992).

The precast wall panels will act as both façade and also structural member that carry the weight from the slab panels above. No horizontal interface is provided between the top and bottom wall to restrain them from sliding against each other. The walls are connected to columns at both ends by shear keys and dowel bars. The distribution of dowel bars would follow the numbers of shear keys provided, with one dowel bar protruded from the wall side spaced at each shear keys. Meanwhile, the size of the shear keys were already prefixed for standardized production having root area of 30150 mm² (201 mm height x 150 mm thickness of wall). The selection of dowel bar diameter depended on combination of both required anchorage length and bar contact surface area as stated in BS 8110-1997, as shown in Eq. (1). Wet concreting is required to cast the column at site using innovated reusable mould (Tiong *et al.* 2011) to reduce cost of formwork.

$$V = 0.6F_b \tan \alpha_f \quad (1)$$

Where V = ultimate pullout force; F_b = anchorage values of reinforcement; α_f = internal friction between the interfaces

3.1 Calibration of the finite element model (FEM)

This study adopted mainly finite element modeling as the main methodology. A finite element modeling method was proposed in this study to numerically represent the interface between wall and frame (column) element. It was anticipated that most nonlinear behaviour of the HCPS would be governed by the stresses and relative deformations that occur at the interface between the



Fig. 3 Full scale HCPS model for lateral cyclic loading test

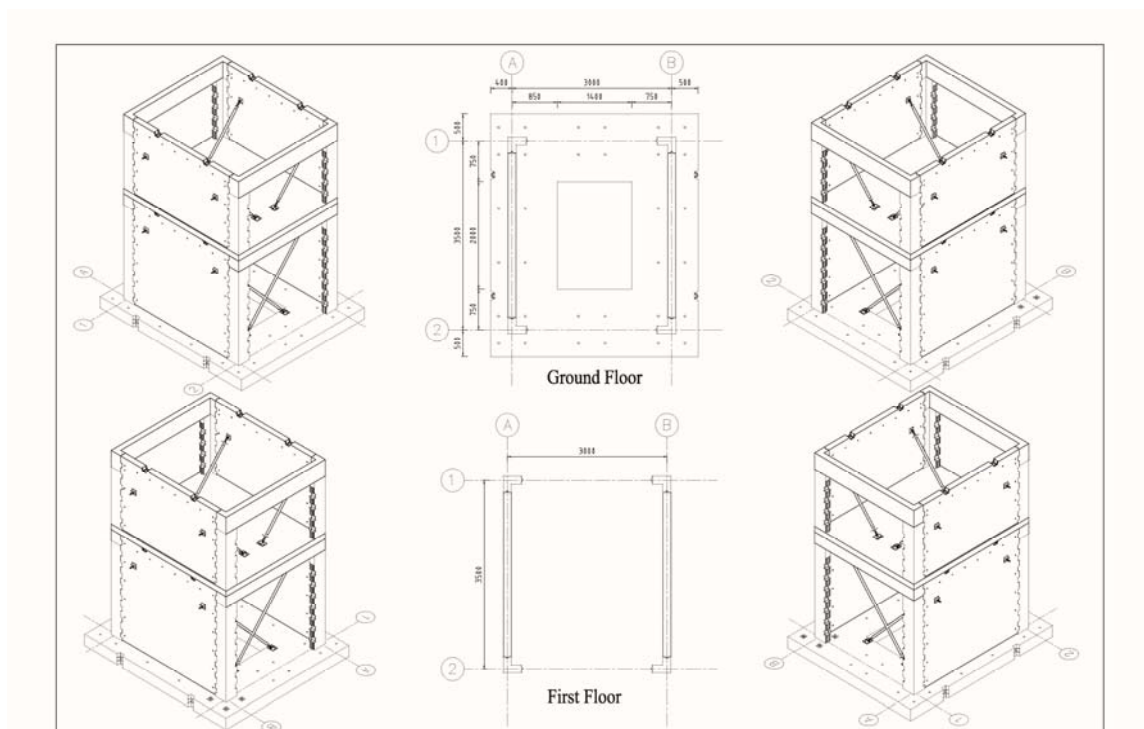


Fig. 4 Layout of the full scale test model

columns and precast panel. This impeded modeling of the interface using conventional rigidly-fixed node.

Calibration of the numerical model was carried out prior to detailed analysis to ensure the accuracy of the computer model. In order to do so, an identical double-bay, two-storey building was casted using the precast wall system (Fig. 3). Layout of the test model is shown in Fig. 4 and

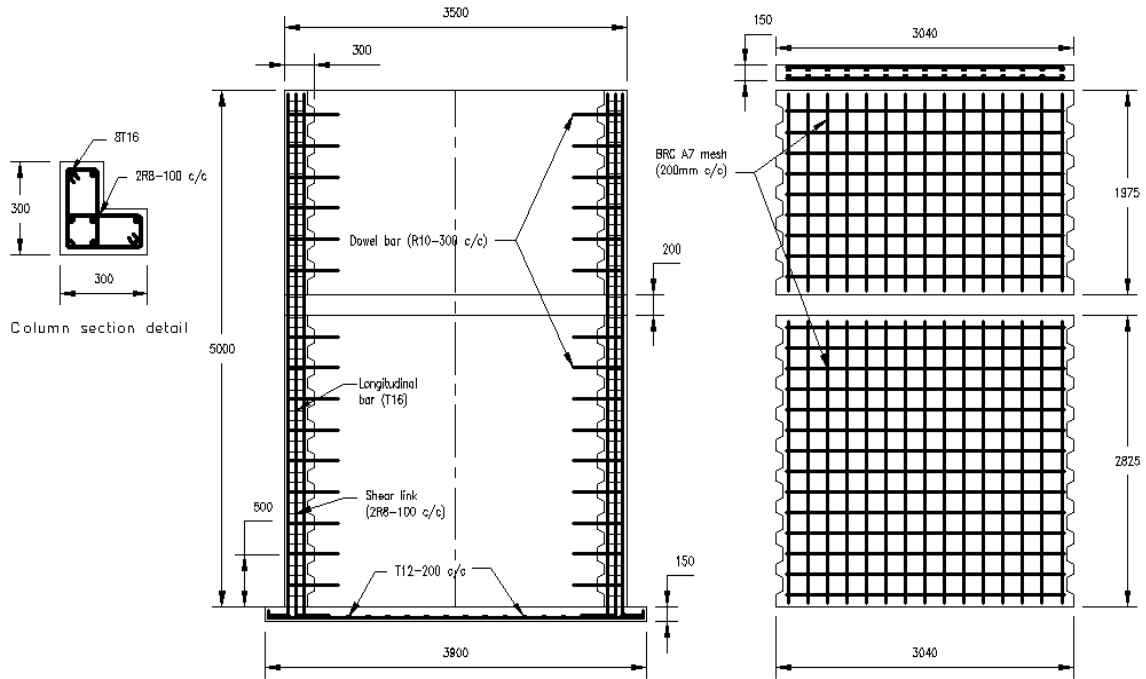


Fig. 5 Structural detailing of HCPS test model

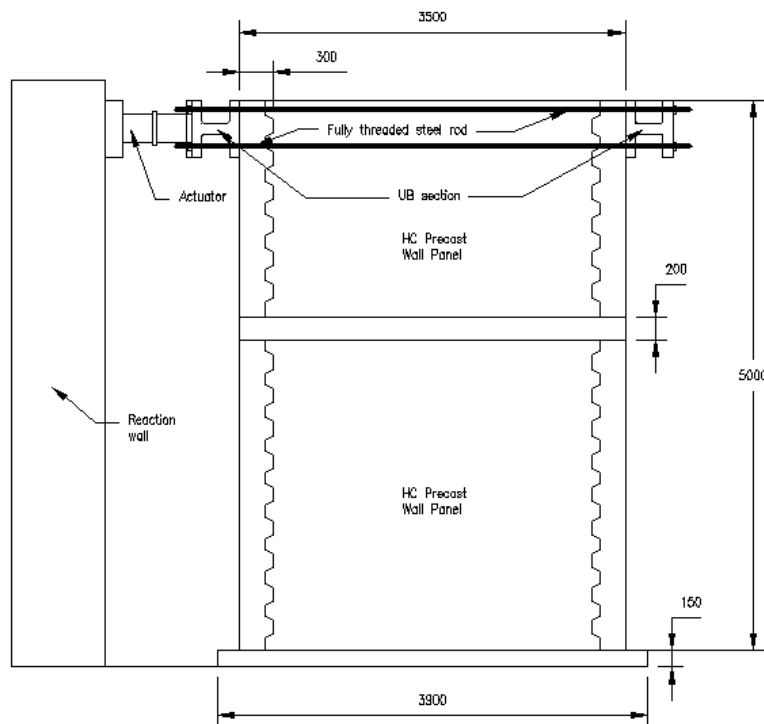


Fig. 6 Laboratory set up for lateral cyclic test of HCPS

Table 1 Structural details of the full scale HCPS test model

Element	Section (mm)	Longitudinal Rebar (mm)	Shear Link (mm)
Wall (upper storey)	150 (t) x 3350 (w) x 1975 (h)	2 layers of BRC A7	Not provided
Column (upper storey)	300 (t) x 300 (w) x 1975 (h)	8T16	2R8-100 c/c
Beam (upper storey)	150 (t) x 450 (d) x 3000 (l)	2T12 (T) 2T12 (B)	R8-150 c/c
Wall (lower storey)	150 (t) x 3350 (w) x 2825 (h)	2 layers of BRC A7	Not provided
Column (lower storey)	300 (t) x 300 (w) x 2825 (h)	8T16	2R8-100 c/c
Beam (lower storey)	150 (t) x 300 (d) x 3000 (l)	2T12 (T) 2T12 (B)	R8-150 c/c
Concrete	Compressive strength = 30 N/mm ²		

the structural detailing can be found in Fig. 5. The temporary struts (found in Fig. 4) that were used to hold the precast wall panels during structure assembling would be completely removed before the testing commenced.

Each side of the five meters tall, double storey building comprised a precast wall panel at each floor level. The building was exposed to displacement-controlled lateral cyclic loading applied at the top of structure. The hysteresis lateral-force deformation curves of the structure were plotted at roof drifts of 0.05%, 0.20%, 0.40% and 0.50%. Laboratory setting up of the testing is illustrated in Fig. 6. It is worth mentioning that the longitudinal reinforcement bars within the cast-in-place columns were continuous along the height of HCPS without any overlapping required. Structural detailing of the test model is listed in Table 1. More details of the experimental are reported elsewhere (Hamid and Mohamed 2011).

The proposed FEM resolved into detail the interface made by shear key and dowel bar into basic reaction forces, as shown in Fig. 7. The shear key protruded along the height of column would mainly be taking all gravitational (vertical) loading from the wall panel. This was represented by a rotational spring element with highly rigid moment-rotation behaviour. Next, the dowel action was assumed to be responsible for resisting all tensile pulling force between the wall and column. Hence, a translational nonlinear link (without having any rotational capability) was assigned to represent the dowel actions. The maximum pullout force (anchorage) of dowel bar was estimated using Eq. (1) while the deformation of normal rebar under tensile stress was based on Bljoger (1988). The plastic behaviour of dowel reaction was represented by means of the force-deformation relationships based on the bi-linear model (Fig. 8). Considering that upon reaching maximum pullout capacity, the dowel bar has very minimal residual strength to resist further tensile force; a sudden drop of strength (130 kN/mm) was assigned as the post-yield stiffness. Another nonlinear link element was also introduced to represent the shear key contact surface or interface between the precast panel and column members. While this surface would purely be attributed to plain concrete, the weak tensile strength of the concrete was modeled assigning hook element and the compressive strength of concrete shear key included potential shear failure of the element (Soudki *et al.* 1996). The ultimate concrete tensile and crushing (or failure in shear) stress was converted into maximum permissible force by multiplying the area of shear key in contact.

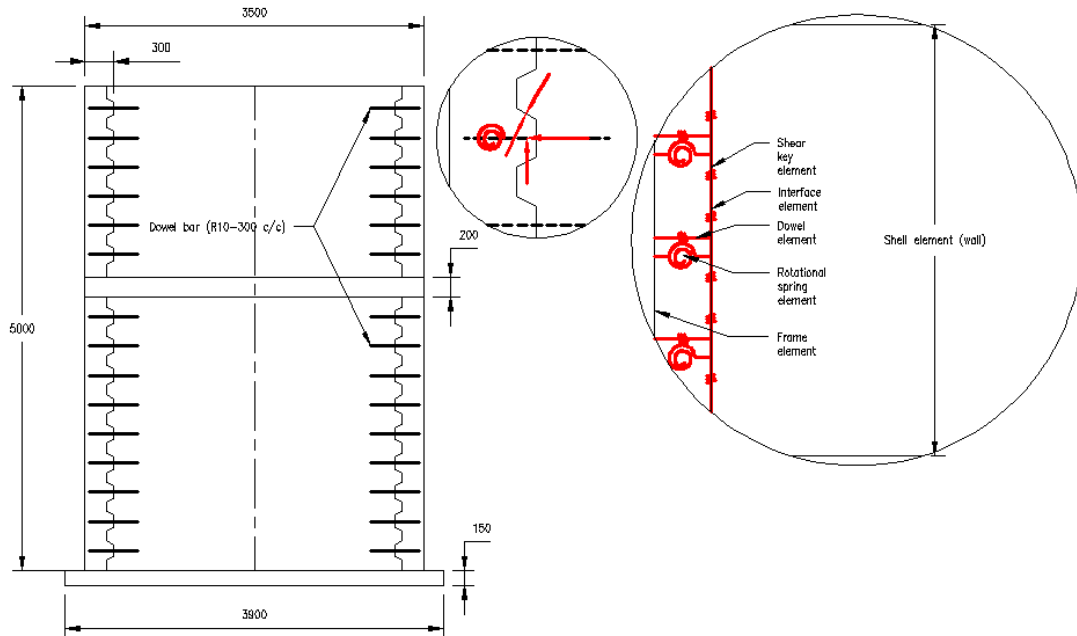


Fig. 7 Assigned nonlinear elements in FEM to represent wall-column interfaces

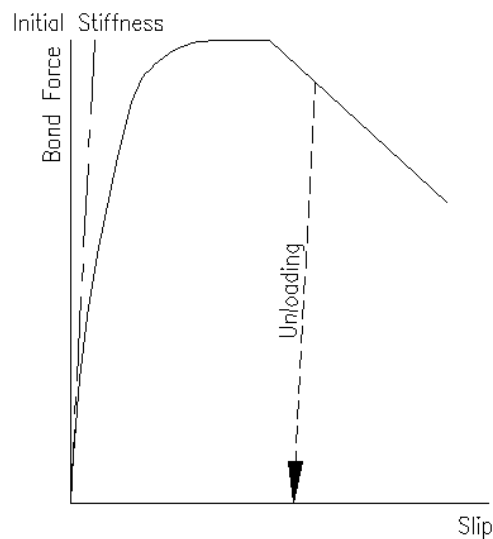


Fig. 8 Hysteresis model for dowel actions (Hashemi *et al.* 2009)

Material property of concrete is governed by its quasi-brittle behaviour and is well known for its relatively higher compressive strength as compared to its tensile capacity. The nonlinear stress-strain property of the concrete needed to be estimated as no data was available. Empirical equations proposed by Desayi and Krishnan (1964), as well as Gere and Timoshenko (1997) were

used to construct the stress-strain model for the concrete material based on uniaxial compressive test results (f_c') and elastic modulus (E_c). While values of uniaxial compressive test strength (f_c') were readily obtained from cube test results, the values of elastic modulus (E_c) and ultimate tensile strength (f_r) needed to be estimated by using Eqs. (2) – (5) as follow (American Concrete Institute 1999):

$$f_c' = \frac{E_c \varepsilon}{1 + \left(\frac{\varepsilon}{\varepsilon_0}\right)^2} \quad (2)$$

$$\varepsilon_0 = \frac{2f_c'}{E_c} \quad (3)$$

$$E_c = 57000f_c' \quad (4)$$

$$f_r = 7.5\sqrt{f_c'} \quad (5)$$

where all units are in psi

ε_0 = strain at ultimate compressive strength and ε = strain other than ε_0 .

3.2 Localized wall cracks

The wall panels were observed to suffer minor cracks, with the largest part of these cracks being concentrated at corner regions of the wall panels (shown in Fig. 9). From the finite element models, these cracks were most probably non-structural cracks that were caused by the weak nature of concrete in resisting internal tensile stresses. Although mesh reinforcements were provided within the wall panels, these reinforcements were only effective in resisting out-of-plane bending moments as well as axial and shear force acting in-plane. The clear concrete cover to the first reinforcement layers was unreinforced. As a result, the tensile stress acting along this layer of concrete cover needed to be resisted by the plain concrete. Using tensile strength equation, the ultimate tensile capacity of the concrete was estimated to be 3.4 N/mm².

In order to test such hypothesis, the HCPS was analyzed using pushover analysis subjected to single-point loading (SPL) imposed at the roof of the structure (to simulate the laboratory loading condition). The red-dotted region in Fig. 9(a) denotes the highest tensile stress concentration within the wall panel obtained at 35 mm of total roof displacement, which could be accumulated to 3.2 N/mm², 95 % of the concrete ultimate tensile capacity. Compared to the observed cracking patterns during the laboratory test as shown in Fig. 9(b), the location of cracks between the finite element model and laboratory observation was found to be in good agreement.

4. Hysteresis response curves

Hysteresis loops of base shear response versus top displacement of HCPS (obtained from both

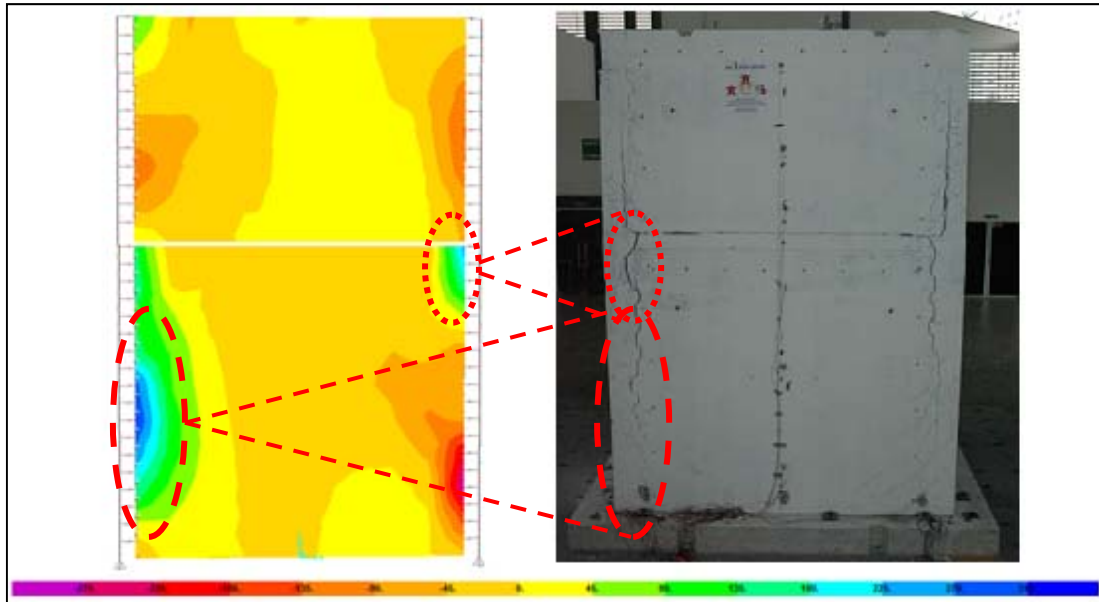


Fig. 9 (a) FEM results and (b) Laboratory observations

experimental work and finite element simulation) are shown in Fig. 10. Studying closely the response curve of HCPS, abnormality was noted particularly in its sudden structural strength degradation (marked by X in Fig. 10). It was clearly observed that most cracks were severely concentrated along the column-wall interface. This separation of the precast wall panel and cast in-situ column should not have caused such a rapid reduction in base shear resistance, instead it should, theoretically be increasing the ductility of HCPS. The pull-out effect of dowel bars protruded alongside the wall panels from column should have dissipated the energy, causing the global period elongation of HCPS.

The rapid decrease causing negative stiffness slope in lateral force resistance of HCPS denoted that critical structural failure must have occurred somewhere (particularly among vertical load-carrying members), and certainly a premature failure. Examining the cracks propagation alongside wall-column interfaces of the tested model, it was found that although the main crack line seems to be separating the wall from column as predicted, the crack propagated into the column itself at the lower section of upper storey (Fig. 11).

Such failure mode of column was not foreseen, and it should not have happened. When HCPS was subjected to lateral loading, the idealized force path should be following through the columns down to the foundation. Flexural failure of column is possible, only if it is unrestrained by any presence of walls adjacent to it. FEMA-356 (Federal Emergency Management Agency 2000) and EC8 clearly state that in the incidence where infill wall is taken into analysis and design of column, the most possible mode of failure should be column shearing at discontinuity interface between upper-to-lower wall panels. Therefore, it has become apparent that the column should either fail in flexure (if unrestrained by any wall), or shear (if vice versa). At worse, axial compression would cause crushing of concrete section at column ends. Nonetheless, none of these failure modes were observed in the laboratory test. Instead, the columns were seemingly to have split into two along the vertical centerline.

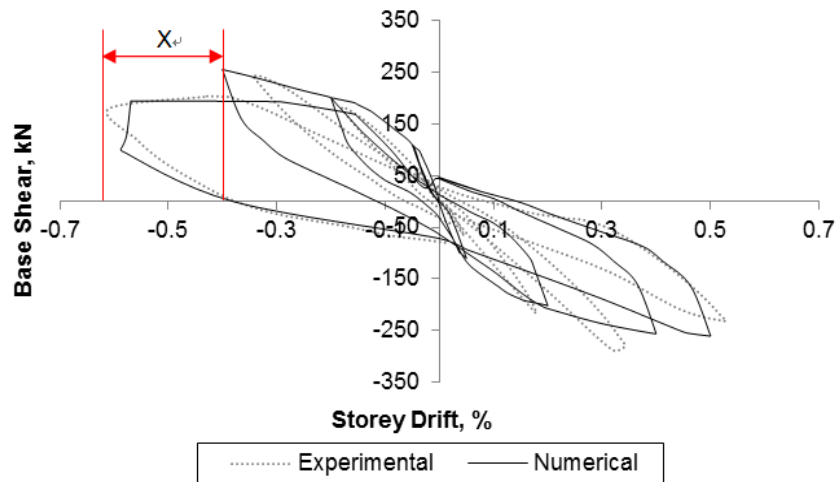


Fig. 10 Hysteresis curves of HCPS from experimental and numerical modeling

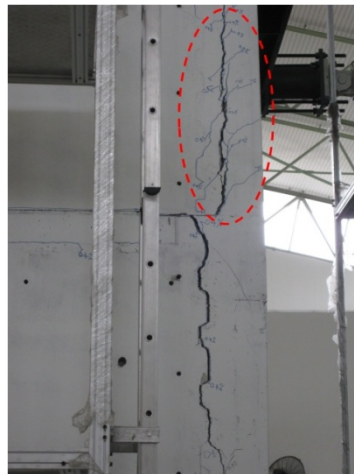


Fig. 11 Splitting of column section

Besides nonlinear deformation observed within the dowel pull-out actions, the global stiffness reduction of HCPS was also attributed to energy dissipation observed in both the shear stresses and relative deformation at the interface. While most of the nonlinear plastic deformation was caused by possible shear sliding between the interfaces (due to lower tensile bonding of concrete), the shear keys at bottom storey were subjected to potential shear failure due to high resultant internal stress.

4.1 Effect of interface stiffness

Reason for such sudden structural strength degradation was investigated by creating finite element modeling of three geometrically identical structures as the experimental test. One of the models possessed rigid wall-to-column interface, namely HCPS-R. In this type of interface, only

the axial deformation (in-plane) of the dowel action was restricted. The remaining two models; namely HCPS-S as well as HCPS-L had semi-rigid interface, and loose interface respectively. Meanwhile, both semi-rigid and loose interface possessed bi-linear force-deformation stiffness with initial stiffness ratio of 18.5 (HCPS-S to HCPS-L). It was worth mentioning that in all the three models, the out-of-plane deformations of the interface were restricted in axial and shear to prevent numerical instability of the model. Such assumption was made as it was not included in the objective of this paper to investigate the out-of-plane behaviour of HCPS.

Graphical plots of the pushover analysis for the three models are shown in Fig. 12. The pushover results revealed that over-designed wall-to-column interface as in HCPS-R caused the non-ductile columns to suffer sudden collapse, due to local plastic hinge formation at the supporting column members. Since the dowel actions were restricted to dissipate any energy, the columns would be the first member to yield at 0.6% storey drift. Dissimilar to such behaviour, semi-rigidly connected wall-to-column structure (HCPS-S) however reflected higher ductility besides demonstrating gradual stiffness hardening. The ultimate lateral displacement of both HCPS-S and HCPS-L was associated with total pull-out of the dowel bar (which caused a significant gap of opening along the interface). In the case of HCPS-L where the interface was over-loosened, the ductility once again decreased. Hence, it's revealed that maximum ductility of HCPS could be reached by providing the optimum interface semi-rigidity and not the most rigid interface as what is thought to be theoretically logic. Since the column of HCPS was not detailed for ductile behaviour, failure of the member would mostly be brittle, leading to sudden strength degradation at yielding point. Therefore, by shifting the brittle failure of column to a gradual type of damage (in this case the separation of wall and column along the interface) provided longer time for evacuation and also such structural damage would not cause immediate failure of the whole system.

The effect of interface stiffness was not investigated prior to the laboratory test (as the initial hypothesis of the laboratory work was stronger interface would produce better seismic behaviour of HCPS). In other words, the interface was constructed to be as rigid as possible; expectantly this

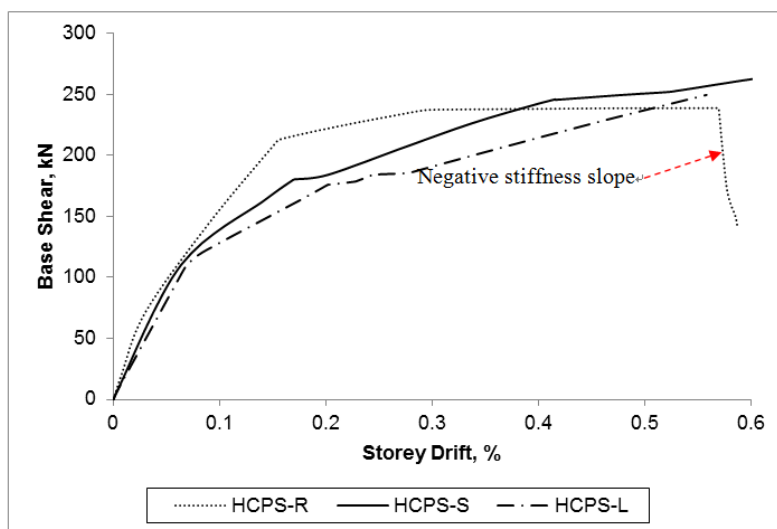


Fig. 12 Capacity curves of HCPS due to different wall-to-column interface stiffness

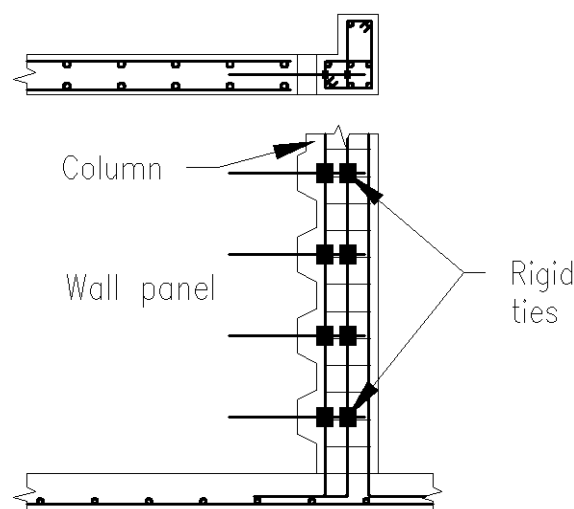


Fig. 13 Additional rigid ties between dowel bars from wall panel and column longitudinal rebars

would increase the overall strength of HCPS. As a result, additional ties (Fig. 13) were provided between protruded dowels bars from the wall sides and the longitudinal reinforcement bars within the columns (only at the upper walls) during the installation of wall panels for the experimental work. This contributed to fully rigid dowel interface (as estimated by initial hypothesis prior to the laboratory test) between the precast panels and column members. Due to the fact that length of protruding dowel bars was only 250 mm, it could not reach the other end of the 300 mm-wide column. Therefore, only one side of the longitudinal column reinforcement was tightened to the dowel bars. Such additional anchorage of bars made the HCPS weaker in resisting severe lateral loads. This extra tightening did not only limited local deformability of the wall-column interface, but it also caused imbalance shear requirement to the column when the wall panels tend to move away from the columns. Thus, stiffness degradation occurred at higher base shear due to column spalling but not hinging when the non-ductile column (which was not designed for any ductility requirement) moved together with the wall panels.

In non-ductile seismic design of structure, it is most desirable to consider strong-column-weak-beam design philosophy for seismic resistance of structures (Lopes and Bento 2001, Mosley *et al.* 2007). The main reason is that column members, which may carry high axial (compressive) loads due to the weight of building often yields in crushing mode. Such failure of structural members is abrupt with little minimal signs of early warnings. Contradict to such unstable failure mode of compressive members; beam hinging type of structural failure is preferred and thus much safer. Whilst beam hinging is almost impossible to be achieved in the cast of HCPS since the system has no beam element, the energy dissipation mechanism has to be transferred to the wall-to-column interface rather onto any structural element itself.

5. Global behaviour factor (q_0)

As mentioned previously, although EC8 does recommends a series of documented values in estimating the global ductility for prediction of inelastic seismic base shear of structure, the code

Table 2 Applied pushover forces and naming convention

Loading Pattern	Abbreviation	Reference
Single point load	SPL	Hamid and Mohamed 2011
Uniform distributed load	UDL	CEN 1998, Pecker 2007, FEMA 2000
Modal distributed load (1 st mode)	MDL	CEN 1998, Kalkan and Kunnath 2006, Chopra 2007
Triangular distributed load	TDL	Pecker 2007, FEMA 2000

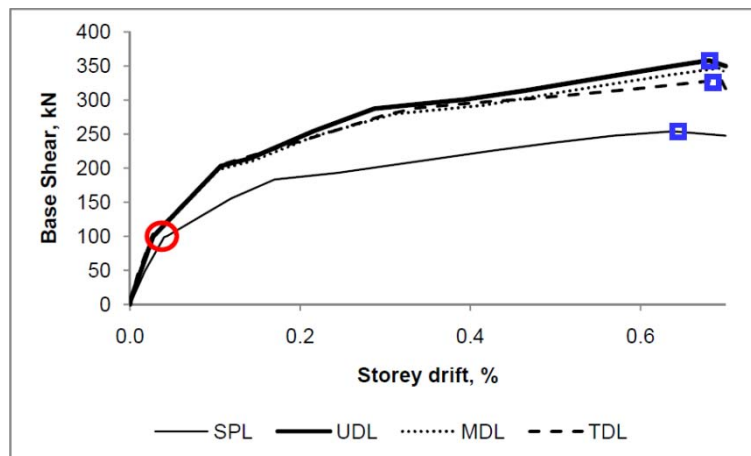


Fig. 14 Capacity curves of HCPS obtained by different pushover load cases

also at the same time suggesting that behaviour factor determined from pushover analysis would be preferred. Therefore, the global behaviour factor (q_0) for HCPS was investigated based on pushover analysis. A total of four different pushover load patterns would be used to determine the capacity curves of the HCPS, as listed in Table 2. The structure was pushed until it reached its ultimate lateral deformation capacity. Since the expected structural damage at its peak lateral displacement would be occurring at the interface, using measurements of the interface gap opening (due to dowel pull-out) as controlling criteria in determining the ultimate displacement capacity would be appropriate. The separation gaps between columns and wall along the interface were measured along the height of HCPS in the laboratory tests, and the structure became unstable when the opening gap was above 7 % of the dowel length. This value was used in the pushover analyses as the target lateral displacement.

The capacity curves of HCPS obtained from the pushover cases as stated in Table 2 were plotted in Fig. 14. The behaviour factor (q_0) for all the four different lateral loading patterns were obtained by normalizing the ultimate (peak) global base shear response (formation of global plastic mechanism which was marked by blue rectangle box in Fig. 14) by corresponding initial yielding (marked with red circle in Fig. 14) base shear. The behaviour (or ductility) factor for HCPS was noted to be 2.60 at ultimate storey drift of 0.6 % based on SPL. Meanwhile, at ultimate displacement capacity of 0.7 % for the remaining UDL, MDL and TDL loading criterion, the global behaviour factors were 3.62, 3.53 and 3.24 respectively.

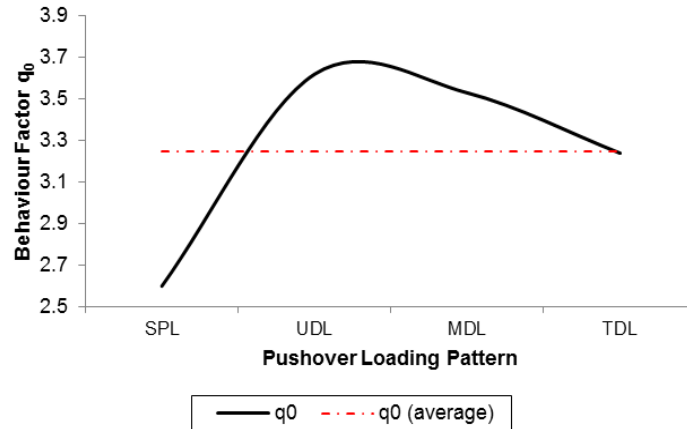


Fig. 15 Values of q_0 for all four pushover loading criterion

Scrutinizing the nonlinear pushover behaviour of HCPS, the values of q_0 were noticed to be dependent on the lateral loading patterns. The types of nonlinear pushover force applied would somehow significantly, affect the ability of HCPS to deform into its plastic region. In other words, the behaviour factor is not a constant value despite the whole structural system itself remained the same. Instead, the characteristic of force applied influenced the nonlinear behaviour of HCPS. Plotting of the q_0 values against different nonlinear loading types is shown in Fig. 15.

As denoted by red lines in Fig. 15 which shows the averaged behaviour factor of q_0 for HCPS, the ductility of HCPS is highest under the UDL pushover pattern, gradually decreasing between the modal pushover and TDL. SPL revealed the lowest ductility behaviour, which was the only one that fell below the average q_0 values approximately by 20 %. Meanwhile the q_0 values, in decreasing order from UDL and MDL pushover patterns would be 12 % and 9 % respectively. Under TDL, the behaviour factor approximated the mean value.

6. Global displacement factor (q_d)

Theoretically, in-plane nonlinear capacity curve of a monolithic concrete wall panel that is designed for plastic hinging at the bottom of the wall is presented in from Eqs. (6) - (11) (Hamid 2009). The idealized capacity curve of the wall panel is divided into three regions. Region 1 is the elastic-linear deformation area while Region 3 describes full-plasticity behaviour of the panel. Region 2 is the intermediate between them.

In Region 1, increment of the horizontal loading from zero to the first loading limit H_r that causes extreme fiber decompression at the lower corner of the wall panel is derived from elastic theory by

$$H_r = (P + W) \frac{l_w}{6H_w} \quad (6)$$

Where

P = gravity load from top of wall

W = self weight of wall panel

l_w = width of wall

H_w = height of wall

Displacement of the wall panel at H_r , which is termed as Δ_r is calculated from

$$\Delta_r = \left[1 + \frac{3}{4} \left(\frac{l_w}{H_w} \right)^2 \right] \frac{H_w}{3E_c I_g} H_r \quad (7)$$

Where

E_c = Young modulus of concrete in N/mm²

I_g = gross second moment area of wall

Upper limit of Region 2 happens when longitudinal reinforcement bars within the wall section begin to yield at yield force H_y that is calculated as follow

$$H_y = K_{ed}(\Delta_y - \Delta_r) + 3H_r \left(1 - \frac{a}{l_w} \right) \quad (8)$$

Where

K_{ed} = wall panel stiffness due to reinforcement

a = position of resultant compression force

At this point of H_y , the in-plane displacement of wall panel Δ_y is derived into Eq. (9).

$$\Delta_y = 2 \frac{f_y}{E_s} L_{ed} \frac{H_w}{(l_w - a)} + \Delta_r \quad (9)$$

Where

E_s = secant modulus of reinforcement bars

L_{ed} = length of longitudinal reinforcement bars

f_y = yield strength of reinforcement bars

In Region 3, stiffness of the wall panel depends largely on the ultimate tensile strength of reinforcing bars. The ultimate lateral force H_u and ultimate lateral displacement Δ_u are then derived as:

$$H_u = K_{ed}(\Delta_p - \Delta_y) + H_y \quad (10)$$

$$\Delta_u = 2 \left(\frac{f_{su} - f_y}{E_s} \right) L_{ed} \frac{H_w}{l_w - a} + \Delta_y \quad (11)$$

Where

f_{su} = ultimate strength of reinforcement bars

Nevertheless, these equations are unlikely to be used for predicting the structural behaviour of precast system such as HCPS due to several factors as follow:

- Failure mode of HCPS is neither due to decompression of lower corner of the structural system nor plastic hinge formation at the bottom section of wall panel, unlike those of monolithic concrete wall panels.
- Presence of dowel actions alongside the HCPS has made theoretical derivation base on elastic theory complicated and almost impractical.

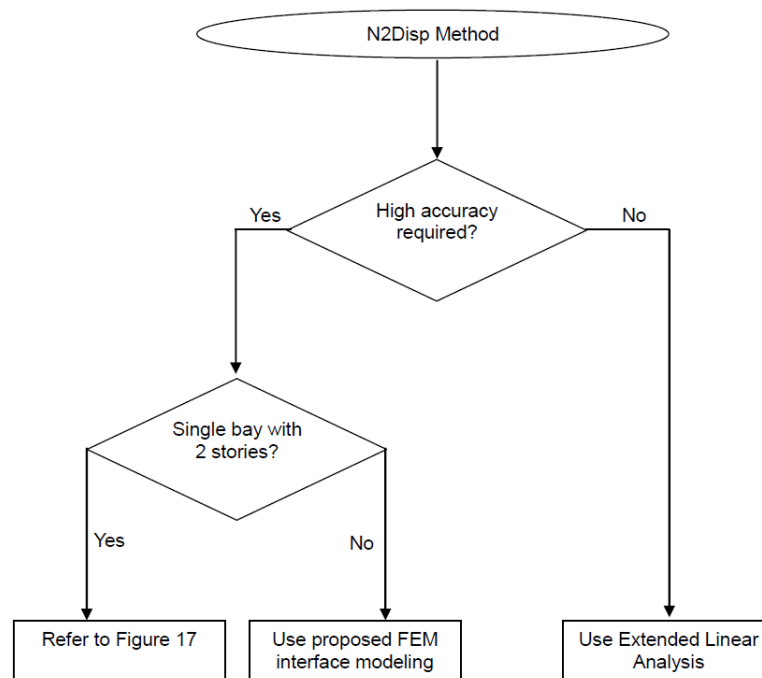


Fig. 16 Procedures using the N2Disp approach

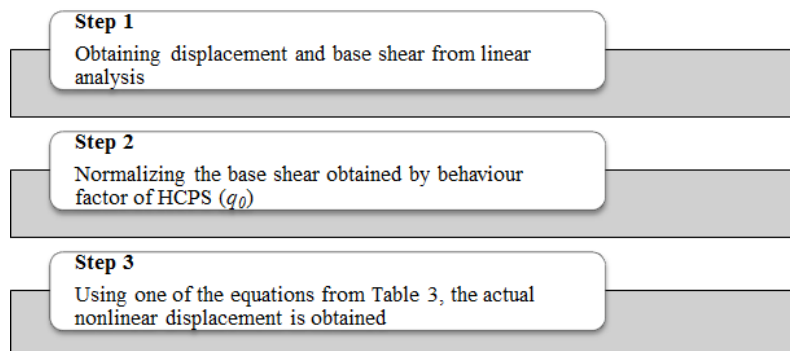


Fig. 17 Simplified steps in using high accuracy N2Disp approach

- The proposed equations required effective stiffness of the wall panel to be known in order for Eqs. (8) and (10) to be used.

EC8 (Section 5.2.2.2) introduces an amplification factor for engineers or designers to estimate the actual nonlinear displacement of a structure based on linear analysis results. Such an amplification factor is denoted as displacement behaviour factor (q_d). The q_d is not only important in estimating displacement of structures in its plastic region, but it might also be used for the preliminary stage in displacement-based design. However, EC8 (Section 5.2.2.2) urges that the value of q_d is to be taken from q_0 . Studying the capacity curves of HCPS in Fig. 12 on the other hand, revealed that q_d being constant was rather unlikely.

Table 3 Equations for high accuracy N2Disp approach

Lateral load type	Elastic base shear range, V_{Eb} (kN)	N2Disp (mm)	Disp. Factor, D_f (mm)
SPL	$V_{Eb} < 260$	No correction	-
	$260 \leq V_{Eb} < 480$	$\Delta = 0.075 \frac{V_{Eb}}{q_0} - D_f$	5.5
	$V_{Eb} \geq 480$	$\Delta = 0.350 \frac{V_{Eb}}{q_0} - D_f$	56.0
UDL	$V_{Eb} < 360$	No correction	-
	$360 \leq V_{Eb} < 1050$	$\Delta = 0.105 \frac{V_{Eb}}{q_0} - D_f$	15.5
	$V_{Eb} \geq 1050$	$\Delta = 0.260 \frac{V_{Eb}}{q_0} - D_f$	58.0
MDL	$V_{Eb} < 350$	No correction	-
	$350 \leq V_{Eb} < 705$	$\Delta = 0.050 \frac{V_{Eb}}{q_0} - D_f$	2.5
	$705 \leq V_{Eb} < 990$	$\Delta = 0.125 \frac{V_{Eb}}{q_0} - D_f$	18.5
	$V_{Eb} \geq 990$	$\Delta = 0.260 \frac{V_{Eb}}{q_0} - D_f$	54.5
TDL	$V_{Eb} < 320$	No correction	-
	$320 \leq V_{Eb} < 660$	$\Delta = 0.040 \frac{V_{Eb}}{q_0} - D_f$	2.5
	$660 \leq V_{Eb} < 900$	$\Delta = 0.140 \frac{V_{Eb}}{q_0} - D_f$	23.5
	$V_{Eb} \geq 900$	$\Delta = 0.420 \frac{V_{Eb}}{q_0} - D_f$	104.0

7. Proposed N2Disp method

In order to improve the accuracy of current practice of displacement estimation as suggested in EC8 (particularly for DCL structure), a new method to obtain the nonlinear displacement of HCPS based on linear analysis result is proposed in this research; which will be abbreviated as N2Disp (New Nonlinear Displacement) throughout this paper. The following steps as shown in Fig. 16 simplified the procedures for using the N2Disp method.

7.1 High accuracy N2Disp approach

Depending on the requirement of analysis, the first two parts of the N2Disp caters for higher accuracy analysis demand. The first recommended method should the structure in consideration happens to be vastly different from the model used in this study, most of the time due to geometry

Table 4 Comparison between EC8 and N2Disp displacement estimation method

Lateral Load Type	Elastic Base Shear, V_{Eb}	EC8	N2Disp	Pushover	EC8 Diff.	N2Disp Diff.
	(kN)	(mm)	(mm)	(mm)	(%)	(%)
SPL	200	1.37	1.52	1.53	-10.78	-0.48
	350	2.34	4.59	4.52	-48.23	1.46
	400	2.70	6.03	5.82	-53.61	3.58
	600	4.07	24.22	22.80	-82.17	6.22
UDL	300	1.07	1.13	1.13	-5.75	-0.30
	750	2.67	5.89	6.00	-55.50	-1.76
	900	3.21	10.24	10.26	-68.71	-0.15
	1250	4.46	30.85	30.68	-85.48	0.55
MDL	250	0.91	0.91	0.91	-0.32	-0.32
	500	1.85	3.16	3.03	-39.04	4.15
	850	3.16	10.72	10.30	-69.29	4.05
	1050	3.91	22.82	21.98	-82.19	3.81
TDL	250	1.13	0.99	0.99	14.24	-0.42
	500	2.25	3.49	3.48	-35.34	0.32
	850	3.78	13.26	13.25	-71.47	0.05
	1000	4.50	26.43	27.09	-83.39	-2.42

unsymmetrical, engineers are advised to adhere to the proposed FEM especially in the interface region to obtain better results.

However, should the structure of interest falls within the analysis models used within this study, it is adequate for engineers to follow the steps as listed in Fig. 17. Equations shown in Table 3 were developed by transforming the nonlinear capacity curve of HCPS into a tri-linear (or in some cases quadrant-linear) curve for each pushover cases. Relationship of difference between the linear and tri- or quadrant-linear curves was investigated. It was found out that the differences were not constant, but in fact the values change at each discrete displacement location or base shears forces.

The fact is based on the capacity curves; the slope of the linear region should indicate the initial stiffness of HCPS, K_0 . In elastic analysis, among the many methods that can be used for estimation of initial stiffness of HCPS, the two recommended approaches would be using finite element model (which shown better accuracy) and using empirical formula in EC8 (which produced conservative period estimation). In using finite element analysis, the wall-to-column interface was adequately represented by rigid in-plane element (in which the deformation parallel to the loading direction was restricted). This was true before the interface yielded, which was always the case in any linear analysis. Meanwhile in using the empirical equation suggested by EC8 in estimation of fundamental period, the stiffness could be underestimated by 3 to 4 times than the actual in which fortunately, would lead to conservative estimation of displacement demand.

Basic structural analysis has always indicated that:

$$K_0 = \frac{F}{\Delta}$$

Where

F = Force

Δ = Displacement

In the case of lateral force resistance for HCPS, the initial resistance provided by the structure in resisting applied lateral force depended on the overall stiffness of the structure, which should be same as K_0 . However, a closer look at the slopes difference between the SPL and other loading pattern such as UDL or TDL, the slopes changed moving from one loading pattern to another. Now, the structure itself remained the same throughout these analyses. In other words, instead of depending only on the geometrical parameters of HCPS alone, the lateral loading (F) also affected its global lateral stiffness. This is because although the base shears might be the same between two dissimilar lateral loading patterns, the internal forces being distributed throughout each element within the HCPS might be different. Therefore, analytical (or closed-form) method to obtain the value of K_0 required a lot of detailed yet complicated analysis. This involved complex distribution of internal forces towards all structural elements (walls and columns) as well as every nonlinear dowel actions. The analytical procedures were more compounded when K_0 in the case of HCPS was, mostly in nonlinear stage.

The proposed N2Disp equations as listed in Table 3 were compared to results obtained when using a displacement behaviour factor $q_d = 1.5$. Results of such comparison are listed in Table 4. Percentage of difference between the actual values and estimated ones using displacement factor from EC8 and N2Disp is plotted in Fig. 18.

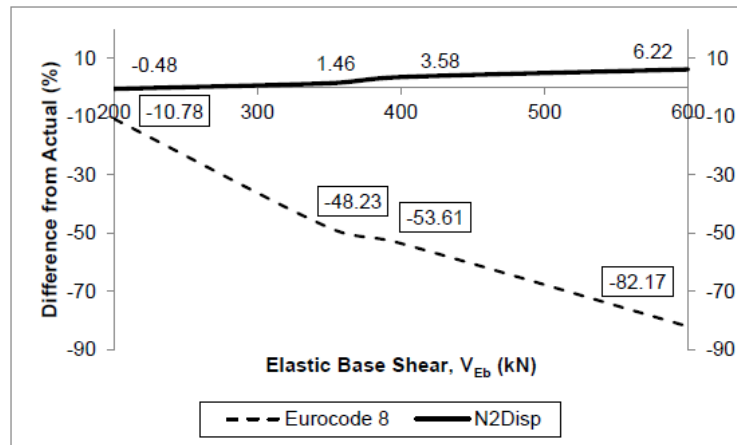
The trend of differences between the actual nonlinear displacement and those obtained through EC8 displacement behaviour factor estimation ranged from minimum of -85.5 % to a maximum 14.3 %. This means that using the displacement behaviour factor as suggested in the current EC8 would usually indicate a lower nonlinear displacement than the actual values. The maximum error was up to 0.15 times lower than the actual value. The differences were observed to be steadily increasing as the base shear increased. This was noted for all types of lateral loadings under consideration except for TDL which reflected slightly higher EC8 prediction in the elastic base shear range. By using the N2Disp method on the other hand, has shown significant improvement in the accuracy of estimating nonlinear displacement based on linear analysis results. The differences were ranging from a minimum of -2.4 % to 6.2 % maximum. The differences were noted to be rather constant regardless of the base shear distributions, except those of SPL and MDL where larger differences were observed at higher base shears.

With the elastic structural analysis indicating that force (F), displacement (Δ) and stiffness (k) is related to each other as shown in Eqs. (12) - (13), such relationship was noted for all four loading cases.

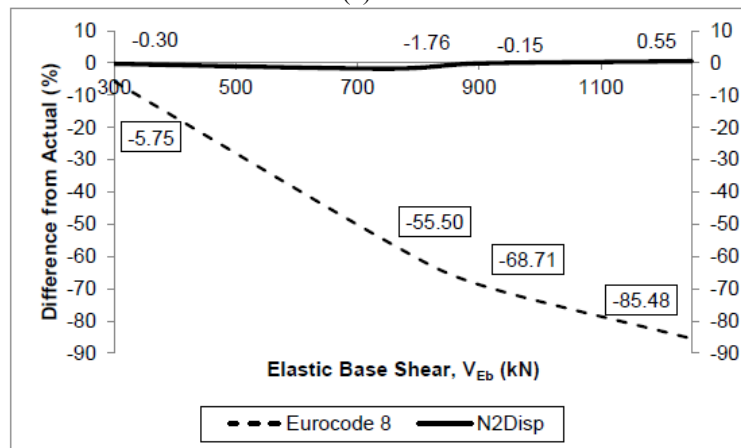
$$F = k\Delta \quad (12)$$

$$k = \frac{F}{\Delta} \quad (13)$$

Nevertheless, the stiffness of a structural system particularly which global stiffness is associated with combinations much relevant local stiffness (in the case of HCPS local interface stiffness, frame stiffness as well as wall flexure, axial and shear stiffness). Frame stiffness can be further categorized into shear stiffness, flexure stiffness and axial stiffness while stiffness associated with wall too has its own classifications. It was not included in the objective of this paper to examine detailed stiffness formulation of the HCPS but rather, the global stiffness of HCPS was formulated from the model responses.



(a) SPL



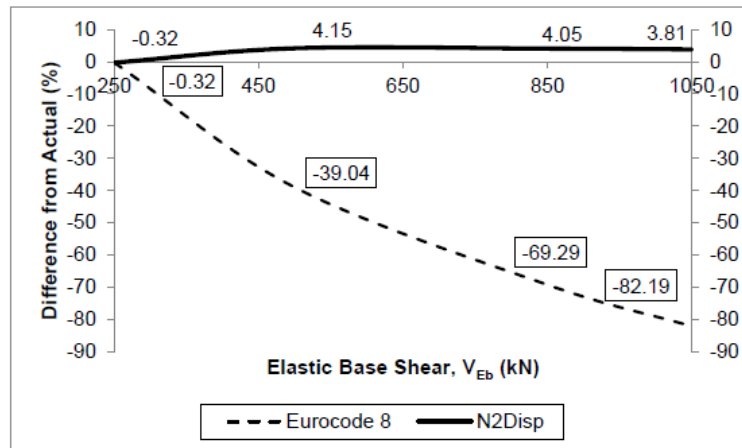
(b) UDL

Fig. 18-1 Percentage difference between actual values with EC8 and N2Disp method – Part 1

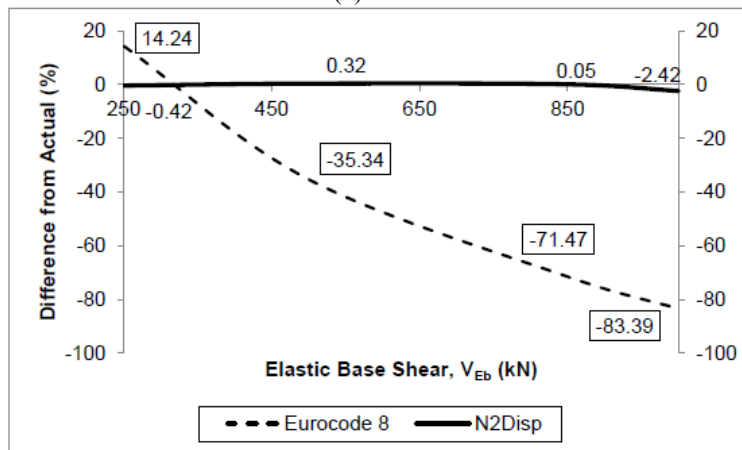
Reviewing the differences between estimated nonlinear behaviour of HCPS based on EC8 and N2Disp methods (Fig. 18), the differences were remarkably significant for higher base shear values (in-plane forces). Therefore, the displacement factor method recommended in the European code is less suitable for displacement estimation of HCPS in regions where high seismicity design is required. The method would over-estimate the global lateral stiffness of HCPS, thus predicting lower displacement value when higher base shear was implicated.

The initial global stiffness of HCPS (linear deformation in the first stage), K_0 of MDL has been observed to be the stiffest, with stiffness value of 75.4kN/mm, followed by TDL with 75.3kN/mm, UDL with 71.8kN/mm and SPL which possessed only 49.2kN/mm. At this initial linear deformation stage, the types of lateral loading applied did not affect the lateral stiffness significantly, except of SPL. The structural elements (column, wall and interfaces) were all in elastic-linear deformation stage.

First stiffness degradations were marked as dark grey in Fig. 19, denoted by K_1 . While the K_1 values between MDL and TDL models were approximately similar (20.0 and 25.0kN/mm



(a) MDL



(b) TDL

Fig. 18-2 Percentage difference between actual values with EC8 and N2Disp method – Part 2

respectively), those associated with SPL and UDL were observed to be different. SPL reported 13.3kN/mm while only 9.5kN/mm was obtained for UDL.

MDL and TDL capacity curves possessed tetra-linear relationship, while for both remaining SPL and UDL comprised tri-linear behaviour. The second stiffness degradation, which was only observed in MDL and TDL, was denoted by K_{1-2} and marked red in Fig. 19. The last stiffness degradation for all load cases, K_2 was however, observed to be rather constant between each loading pattern between 2.4kN/mm (minimum) to 3.8kN/mm (maximum).

Such differences of stiffness occurred between each loading pattern happened due to the difference local stiffness being involved due to dissimilar global loading. As mentioned before, local stiffness associated within column members were flexural stiffness, shear stiffness or axial stiffness. Besides frame elements, the interface itself, particularly dowel actions possessed very different stiffness in terms of compression or tensile deformation capability. Under direct tensile stress, pull-out of dowel was possible, while compression leads to shear key fractures or adjacent column shearing possibility. Whilst these local stiffness built up to form the global stiffness of

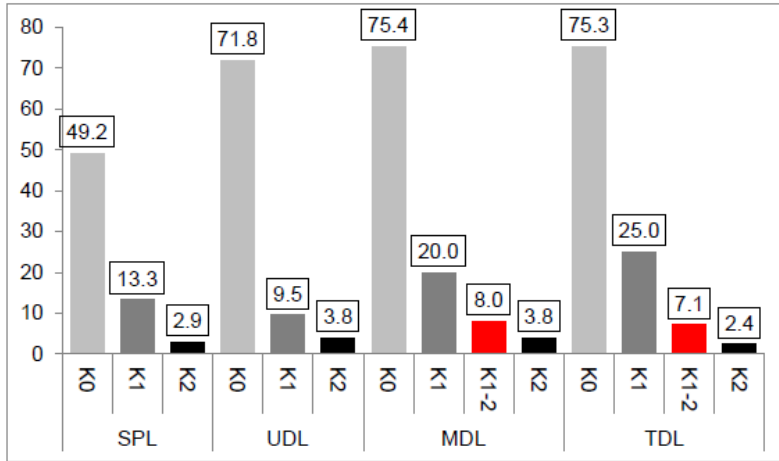


Fig. 19 Stiffness changes of HC Precast System for all pushover load cases

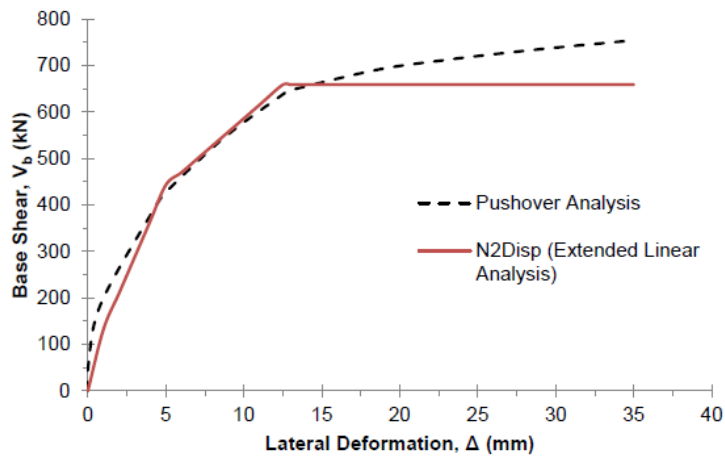


Fig. 20 Extended linear analysis verification with 2 storey 3 bay HCPS

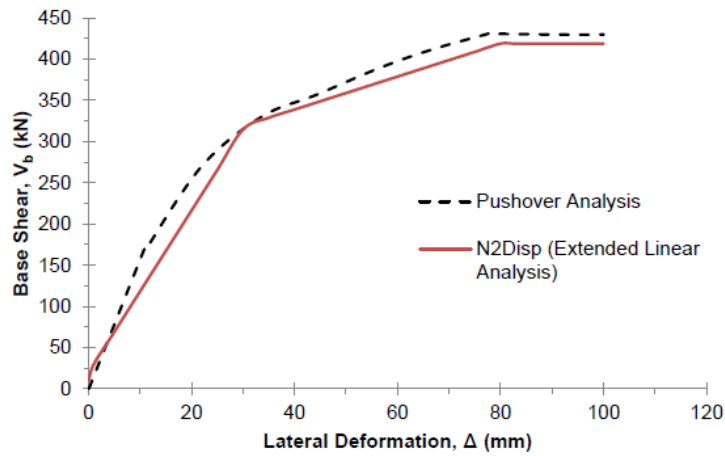


Fig. 21 Extended linear analysis verification with 3 storey 1 bay HCPS

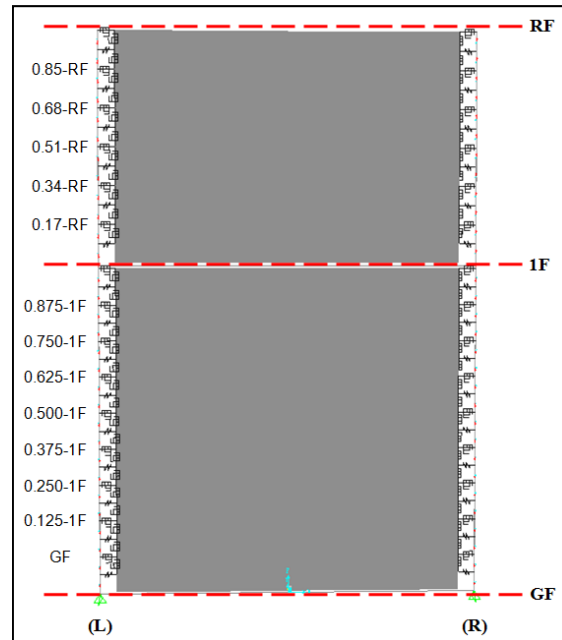


Fig. 22 Numbering and naming convention of dowel bars for HCPS

HCPS in resisting the lateral force applied, a slight change in local stiffness (not because of geometrical or structural modification) but because of different internal load path that called for formation of different stiffness into place affected the global stiffness apparently.

Generally, the global stiffness demonstrated by MDL was noted to be highest amongst the three others. The wall panels were in tensile stress with minimal compressive strut observed at upper storey (1F to RF). Besides that, approximately 75 % of the dowels within this storey level were in tension, with only 25 % in compression. This has shown that in order to achieve higher stiffness, the upper storey of the structure has to be in tensile instead of local compressive deformation. Large compressive strut formed at upper storey (such as in SPL) would lead to less stiffer global behaviour. On the other hand, TDL demonstrated wider compressive strut at the ground storey level (GF to 1F). Global stiffness of HCPS in TDL was the second highest, following MDL.

7.2 Extended linear analysis (approximation) approach

By studying the trend of nonlinear capacity curve of HCPS under the four different pushover loadings as well as its global structural behaviour, its pattern revealed big potential to be generalized in order to estimate nonlinear deformation of any HCPS structure. It was consistently observed that the peak displacement of post-yield region would be approximately 2.5 times the elastic (first) yield deformation. In other words, the ductility of HCPS would be averaged as 2.5, regardless of whatever behaviour factor it may possess. This was higher than the currently recommended 1.5 for DCL structure by EC8.

Thus, a slight modification was made to the current equal-displacement-rule (EDR) where an intermediate effective stiffness would be introduced between the initial elastic and ultimate plastic region in the global capacity curve. This intermediate stiffness, K_2 can be estimated from Eq. (14).

$$K_2 = \frac{V_{Eb} \cdot \alpha_l (q_0 - 1)}{\Delta_l (2.5 - 1.0)} \quad (14)$$

Where q_0 = behaviour factor; V_{Eb} = design base shear; α_l = elastic base shear factor; and Δ_l = first yield displacement

In using this approach, engineers would first get the response of HCPS under any types of linear (i.e. design spectrum or equivalent lateral force distribution) analyses. The capacity of critical structural elements where in the case of HCPS, the columns were checked to ensure they remain in the elastic region. All nonlinearity is restricted to occur within the wall-column interface and within the wall panel itself. Due to the lower stiffness of interface in relation to the in-plane wall stiffness, the nonlinearity response within wall element itself is minimal. Then, by choosing the target behaviour factor, the slope of K_2 was obtained using the proposed equation. The peak displacement of K_2 is limited at maximum of $2.5\Delta_l$. By connecting between these points, the response curve of HCPS can be estimated without the need to perform nonlinear analysis.

This extended linear analysis method was tested and verified by comparing the estimated curves with two pushover results consisting of one single-bay, three-storey HCPS and another triple-bays, double-storey model. The results are shown in Fig. 20 and Fig. 21. It was revealed that the proposed extended linear analysis approach was able to produce good approximation nonlinear deformation of HCPS in comparison to the numerical models.

8. Dowel behaviour

The pushover lateral loads were applied from the left side of the HCPS (denoted by (L) in Fig. 22) for the pushover analysis. Therefore, the frame elements alongside (L) should be in tension whilst the (R) columns in compression, generally. The dowel axial actions were studied in detail to investigate the distribution of internal forces alongside the HCPS as well as the effective diagonal strut-and-tie relationship within the wall panels.

The dowel actions from the bottom of (R) side up to 0.375-1F were in compression for all lateral load cases. At these points of dowel action, the largest axial compression was noted at GF level; slowly decreasing when moving up to 0.375-1F level. The highest dowel compression for GF was observed to be ranging between 94 to 99 % of base shears for SPL, UDL, MDL and TDL. The dowel compression built up to such maximum values before decreasing nonlinearly. Interestingly, the dowel action at 0.500-1F was detected to be in dual-mode depending on the lateral loading type. For all the three lateral load types except TDL, the dowel axial at this point was in tension. This significantly proved that the width of the diagonal compression strut was not constant, as which was proposed by Elliot (2002). Besides the structural geometry and stiffness property alone, the types of lateral load applied onto the structure would, in this case cause the HCPS to possess different effective-strut-width.

Apart from TDL load case, the other lateral load patterns have yielded dowels from 0.500-1F to 1F to axially be in tension. Unlike the dowel compression behaviour as discussed previously, the tension behaviours of these dowels were found to be irregular between lateral load cases. Under the SPL, the tension increased proportionally to the base shears, in nonlinear relationship. However lateral excitation by the UDL have loading pattern have caused the tension forces within the dowels increased exponentially at the very initial base shears and reached their peaks approximately at 2 % (8 kN) of ultimate base shear value (360 kN); for 0.750-1F, 0.875-1F and 1F

levels. Besides that, the distributions of such tension forces were not perfectly proportionate to along the height. In fact, higher tension requirement was found at 1F and 0.750-1F, while in the midst of these two (0.875-1F) possessed relatively the lowest internal force. Not only the effective width of compression diagonal strut was found to be non-constant, but such characteristic of the tension strut was also observed.

For levels between 1F to RF, the dowels in compression were found to be independent of lateral loading types, except for those induced by SPL. The SPL have caused three dowels to be yielding compressive axial forces, namely the 0.17-RF, 0.34-RF and 0.51-RF respectively in the descending order from largest value to lowest. The other three remaining lateral loads have seemingly to be causing compression only in two dowels; the 0.17-RF and 0.34-RF. Among all the four load cases, the SPL caused largest compression requirement (in dowel 0.17-RF) by nearly twice as much as induced by the remaining three. Therefore once again, the diagonal strut in compression at this upper story (1F to RF) was not the same between SPL and the other load types.

The last part of dowels in tension for the (R) side was those along 0.51-RF (except for SPL) to RF, including between them 0.68-RF and 0.85-RF. The nonlinear tension behaviours within these dowels were found to be rather similar to those tensile dowels at lower storey. The SPL was imposing largest tensile demand onto the RF level, resulting in nearly 6 % of base shear demand of dowel tensile requirement. On the other hand, the UDL, MDL and TDL required approximately between 2.5 to 3.5 % only, about twice as low as SPL would have required.

For the (L) side, the bottom dowels at GF up to 0.625-1F were in tension, except for TDL in which 0.625-1F was in compression. This revealed that at least five of the eight dowels in the lower storey were in tension, as compared to only four on the (R) side. Highest tension demand was noted in GF under UDL loading type, which resulted in 32 % of base shear demand in tensile. The other loading cases required tensile dowel forces below 13 % at the same GF level. Moreover, unlike the other behaviours of dowel in tensile as discussed previously for the (R) side, the high tension demands occurred at very initial stage of all lateral loadings for the (L) side. The tensile stresses built up rapidly initially, reaching their peaks below 50 kN of base shears, followed by swift reduction until 100 kN, and then gradually increasing as the base shear continued rising.

The dowels at 0.750-1F, 0.875-1F and 1F were in compression, with the highest compression demand noted at 1F. In the TDL case, 0.625-1F was also in compression, besides the earlier three. Compression actions in 1F were observed to be increasing vastly at initial base shears and gradually decreasing until the ultimate base shear. However, such behaviours were not noted in other dowels. Instead of gradually decreasing, compressive stresses continued to build up in these dowels until higher base shear compared to 1F.

The tensile stresses requirement along the upper storey on (L) side frame differed significantly under each lateral loading pattern. Both SPL and UDL have caused dowels at 0.17-RF, 0.34-RF and 0.51-RF to be in tension mode, while witnessed in the MPL case was that 0.68-RF and 0.85-RF were added to the group. However, only two dowels, namely the 0.17-RF and 0.34-RF were in tension under TDL execution.

The same discrepancy of dowel actions was also noted for compressive stresses at the (L) upper storey. The SPL and UDL case caused four dowels, namely the 1F, 0.68-RF, 0.85-RF and RF to be compressed. Highest compressive stress demand was at the RF level. Nonetheless under the MPL pattern, only 1F and RF were in compression and yet five dowels (1F, 0.51-RF, 0.68-RF, 0.85-RF and RF), were noted in TDL study.

Meanwhile, the dowel actions along (L) side should supposedly be exactly opposite to every single dowel forces on the (R) side corresponding to the same height levels. This should be the

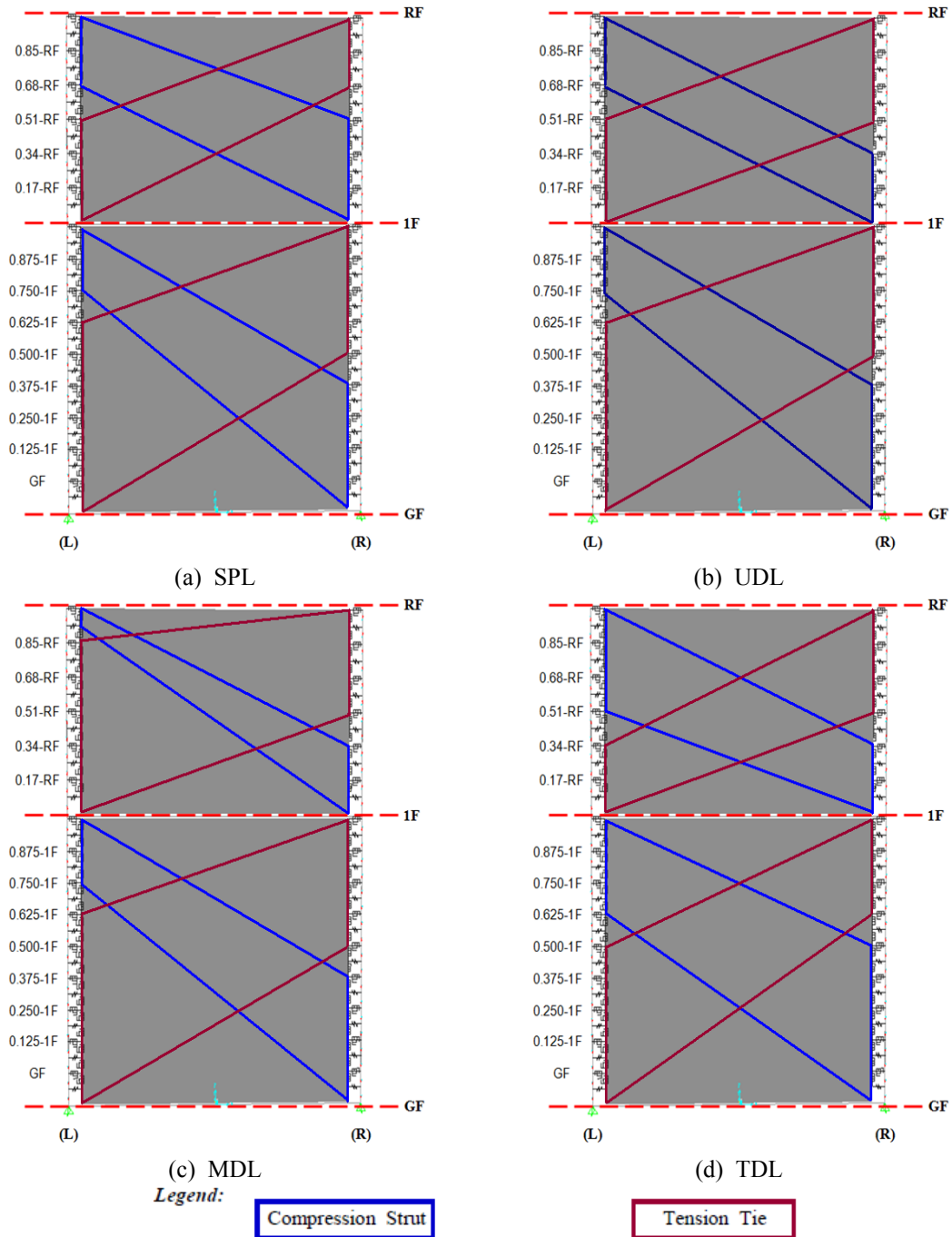


Fig. 23 Diagonal compression and tension strut-tie width under different pushover loadings

case in order to idealize the constant width of strut theory. However, such idealized behaviour was not reflecting the true behaviour of HCPS, as what was observed in this study.

Moving on from the (R) to (L) side, the dowel actions were not symmetrical to their corresponding location between the two sides. Such observations revealed the high potential of asymmetrical have occurred within the HCPS, which was symmetrical in geometrical as well as stiffness parameters. As a result, should the structural analysis have to be done using the strut-and-tie model instead of the wall element itself, the effective widths of the strut-and-tie model should be properly addressed (Fig. 23).

Such varying nature of the diagonal compressive and tensile strut-tie behaviours has also indicated the dynamicity of neutral axis within the wall panels, despite maintaining the same geometrical aspects. Except for MDL case, the neutral axis of the wall panels at upper storey was noted to be rather constant for the three other lateral load patterns. The MDL has witnessed complicated neutral axis. At lower storey, neutral axis location observed TDL were consistent, but neither for SPL, UDL nor MDL.

5. Conclusions

In this study, the nonlinear performance of an innovated non-ductile precast concrete wall system (HCPS) was investigated using pushover analysis. The numerical (finite element) model used in the study was calibrated with full-scale experimental work prior to being used in the parametric study. Based on result observations and data analysis, the following conclusions were drawn:

- The proposed FEM for nonlinear wall-column interface element was able to generate global force-deformation hysteresis curves that were in good agreement to the laboratory lateral cyclic loading observations of HCPS.
- Ductility of non-ductile structure such as HCPS was increased by providing optimum interface stiffness possessing semi-rigidity instead of either fully rigid or flexible interface. In the case of HCPS, over-tightened dowel actions between the precast wall panel and column led to premature column splitting.
- The ductility (behaviour) factor q_0 of HCPS ranged from 2.60 to 3.62. These factors were not constant despite geometrical and structural aspects of HCPS remained identical throughout the analyses. Hence, the types of applied pushover load patterns influenced the effective stiffness of HCPS, thus affecting its deformability.
- N2Disp method was proposed for designers to accurately estimate nonlinear deformation of HCPS through linear analysis. For this particular case of the system under consideration, the results obtained by the use of N2Disp approaches, were found to be more accurate than the ones for behaviour factor $q_0 = 1.5$.
- The strut-tie width of wall panels under compression and tension is depending on the lateral loading pattern. Hence, a fixed width of such strut-tie model is not advisable.
- Engineers and designers should not be taking the current international seismic design guidelines for granted in the case of low ductility design process. Particularly should the seismic demand falls into the region in between post-elastic (yield) and ultimate capacity in the equal displacement rules.
- For DCL structure mainly such as HCPS, the processes between structural modeling, design and

construction must be cautiously implemented to ensure higher degree of similarity. It was clearly revealed in this study that merely by providing additional rigidity between dowel bars and rebar within columns (which was made worse by imbalance ties), the local failure mode and global behaviour of the structure was significantly affected.

Acknowledgments

The research described in this paper was financially supported by the Construction Industry Development Board of Malaysia through research VOT 73750. Laboratory specimen preparation by HC Precast System P/L and also testing facility provided by the Construction Research Institute of Malaysia were also acknowledged.

References

- American Concrete Institute (1999), *ACI 318: Building code requirements for reinforced concrete*, Farmington Hills, Michigan, American Concrete Institute.
- Bljucer, F. (1988), *Design of precast concrete structures*, West Sussex, England, Ellis Horwood.
- British Standards Institution (1997), *BS 8110: Structural use of concrete. Part 1-Code of practice for design and construction*, London, British Standards Institution.
- CEN 1992 (2002), *Eurocode 2: Design of concrete structures – Part 1: General rules and rules for building*, London, UK, British Standards Institution.
- CEN 1998 (2003), *Eurocode 8: Design of structures for earthquake resistance - Part 1: General rules, seismic actions and rules for buildings*, London, UK, British Standards Institution.
- Chakrabarti, S.C., Nayak, G.C. and Paul, D.K. (1988), “Shear characteristics of cast-in-place vertical joints in story high precast wall assembly”, *ACI Struct. J.*, **85**(1), 30-45.
- Chopra, A.K. (2007), *Dynamics of structures-theory and applications to earthquake engineering*, New Jersey, US, Pearson Prentice Hall.
- Christiansen, J.V. (1973), “Analysis of lateral load resisting elements”, *PCI J.*, November-December, 54-71.
- Desayi, P. and Krishnan, S. (1964), “Equation for the stress-strain curve of concrete”, *J. Am. Concrete Inst.*, **61**, 345-350.
- Divan, M. and Madhkhan, M. (2011), “Determination of behaviour coefficient of prefabricated concrete frame with prefabricated shear walls”, *Procedia Eng.*, **14**, 3229-3236.
- Elliot, K.S. (2002), *Precast concrete structures*, Woburn, MA, Butterworth-Heinemann.
- Englekirk, R.E. (2003), *Seismic design of reinforced and precast concrete buildings*, Canada, John Wiley and Sons.
- Federal Emergency Management Agency (FEMA) (2000), *FEMA-356: Pre-standard and commentary for the seismic rehabilitation of buildings*.
- Frosch, R.J., Li, W., Jirsa, J.O. and Kreger, M.E. (1996), “Retrofit of non-ductile moment-resisting frame using precast infill wall panels”, *Earthq. Spectra*, **12**(4), 741-760.
- Gere, J.M. and Timoshenko, S.P. (1997), *Mechanics of materials*, Boston, Massachusetts, PWS Publishing.
- Hamid, N.H.A. (2009), *Seismic performance and design criteria of precast wall panels*, Malaysia, University Publication Centre UiTM.
- Hamid, N.H.A. and Mohamed, N.M. (2011), “Seismic behaviour of non-seismic precast wall panel of double-storey house under quasi-static lateral cyclic loading”, Technical Report. (Unpublished)
- Haron, N.A., Hassim, I.S., Kadir, M.R.A. and Jaafar, M.S. (2005), “Building cost comparison between conventional and formwork system: a case study of four-storey school buildings in Malaysia”, *Am. J. Appl. Sci.*, **2**, 819-823.

- Hartland, R.A. (1975), *Design of precast concrete*, London, Surrey University Press.
- Hashemi, S.S., Tasnimi, A.A. and Soltani, M. (2009), "Nonlinear cyclic analysis of reinforced concrete frames, utilizing new joint element", *Sci. Iranica Transaction A: Civil Eng.*, **16**(6),490-501.
- Hassim, S., Jaafar, M.S. and Sazalli, S.A.A.H. (2009), "The contractor perception towards industrialized building system risk in construction projects in Malaysia", *Am. J. Appl. Sci.*, **6**, 937-942.
- International Code Council (2009), *2009 International building code*, Illinois, USA, International Code Council.
- Kalkan, E. and Kunnath, S.K. (2006), "Adaptive modal combination procedure for nonlinear static analysis of building structures", *J.Struct. Eng.*, **132**(11), 1721-1731.
- Lopes, M.S. and Bento, R. (2001), "Seismic behaviour of dual systems with column hinging", *Earthq. Spectra*, **17**(4), 657-678.
- Lu, X., Urukup, T.H., Li, S. and Lin, F. (2012), "Seismic behavior of interior RC beam-column joints with additional bars under cyclic loading", *Earthq. Struct.*, **3**(1), 37-57.
- Mosley, B., Bungey, J. and Hulse, R. (2007), *Reinforced concrete design to Eurocode 2*, New York, US, Palgrave Macmillan.
- Pecker, A. (2007), *Advanced earthquake engineering analysis*, New York, US, Springer Wien New York.
- Raths, C.H. (1977), *Design of load bearing wall panels—design considerations for a precast prestressed apartment building*, Illinois, US, Prestressed Concrete Institute.
- Rodriguez, M.E. and Blandon, J.J. (2005), "Test on a half-scale two story seismic-resisting precast concrete building", *PCI J.*, January-February, 94-114.
- Soudki, K.A., West, J.S., Rizkalla, S.H. and Blakett, B. (1996), "Horizontal connections for precast concrete shear wall panels under cyclic shear loading", *PCI J.*, **41**(3), 64-80.
- Tiong, P.L.Y., Adnan, A. and Ahmad, F. (2011), "Improved discrete precast concrete wall panels and modular moulds for wet joints in Malaysia", *Concrete Plant Int.*, **6**, 150-152.
- Vafaei, M., Adnan, A. and Yadollahi, M. (2011), "Seismic damage detection using pushover analysis", *Adv. Mater. Res.*, **255-260**, 2496-2499.